J. Mountain Res. P-ISSN: 0974-3030, E-ISSN: 2582-5011 DOI: https://doi.org/10.51220/jmr.v16i2.22
Vol. 16(2) Special Issue ICRAMS-2021, (2021), 169-181

A Brief Study of Physical Properties of Rf Magnetron Sputtered Azo Thin Films

Richa Sharma[1*] • Fouran Singh[2] • J M S Rana[1]

[1]*Department of Physics, H.N.B Garhwal University, SRT Campus Badshahi Thaul, Tehri Garhwal 249199*
[2]*Materials Science Group, Inter University Accelerator Centre, Aruna Asaf Ali Marg New Delhi 110 067*

*Corresponding Author Email: sharmariccha05@gmail.com

Received: 4.9.2021; Revised: 19.10.2021; Accepted: 28.10.2021

Abstract: We reported the physical properties of undoped and Aluminium doped ZnO (AZO) thin films that were synthesized by the RF magnetron sputtering method on a quartz substrate. The effect of dopant concentration on structure, morphology, optical and electrical properties of the thin films have been studied systematically by XRD, Raman spectroscopy, AFM, FE-SEM, UV-VIS spectroscopy and I-V measurement (two probe method) respectively. The crystallite growth of the thin films is along c-axis (002) orientations with hexagonal wurtzite structure. The crystallinity is enhanced in the 1%AZO thin films as compared to undoped ZnO. The transition of stress value after introducing the dopant is discussed. These changes are further correlated with the observed morphological changes. The alteration in optical transmission and optical band gap is also discussed extensively. For the AZO (1% and 2%) thin films the n-type conductivity and ohmic nature measured by using Keithley two probe set up. The responsible mechanism for improved conductivity is discussed. In the FTIR spectrum the peaks originated by the tetrahedral coordination of ZnO are observed which further confirms the wurtzite structure of the deposited thin film sample that are recorded by the XRD pattern.

Keywords: RF magnetron sputtering, FE-SEM, Raman Spectroscopy, AZO and optical bandgap.

Introduction

The economical, inert and accessible metal oxides have been extensively studied for commercial applications. In the fashion of miniaturization, the study of dimensionality has also been broadly explored by the scientific community for their possible applications such as electrochromic windows(Granqvist, 2000) and optoelectronic devices(Malek et al., 2013; Peiró et al., 2006). The requirement of these high-performance devices is contented by the metal oxide Zinc oxide(ZnO) that have good structural, electrical, optical and electrochemical properties. The resistive stoichiometry of ZnO can be converted to conducting nature by introducing oxygen vacancies that behave as donors with a proper dopant. The group III elements such as aluminium (Al) are chosen as dopant because Al has much smaller ionic radii (0.54Å) as compared to Zn(0.74Å) that can favourably occupy the interstitial(Lee and Park, 2004).

The thin film growth technique and conditions strongly affect the crystal structure. In the past time, researchers are using top-down approaches and methodologies to achieve high-quality ZnO thin films. However, the commercial application oriented devices require a low cost but necessarily with high-

performance and reproducibility. While choosing the appropriate technique as per the requirement a thorough analysis of the external factors should also be considered. The literature of ZnO thin films includes many different thin film deposition techniques. The basic material properties of the ZnO material can be augmented and some functionality could also be added by choosing different deposition techniques in addition to other material tailoring methods (doping, annealing, different substrate and ion irradiation etc.). RF magnetron sputtering is one of such methods to produce good quality thin films that provide controlled composition, homogeneity, great adhesion and control of thin-film thickness. In the fabrication of devices, the present stress/ strain in the AZO thin film is expected to be a critical factor that influences its performance. Though there are already plenty of reports on AZO thin films, relatively a few focus on the effect of the stress/ strain and their correlation with the other material properties. The authors decisively believe that such a study is beneficial to deepen the understanding for the development of high-quality thin films for improved ZnO based devices.

2. Experimental details

The undoped ZnO and Al doped thin films with aluminium content 1%AZO and 2%AZO were deposited using RF magnetron sputtering technique at room temperature on quartz and the silicon substrate. The targets were prepared by employing the solid-state reaction method. A rough vacuum is created in the sputtering chamber by using a rotary pump through a roughing valve. Before introducing the gas in the chamber the pressure of the chamber is brought down to 5.5×10^{-5} mbar. The constant flow of Argon gas in standard centimetre per minute (sccm) is ensured by using MKS mass flow meters. The RF power was maintained at 100W with a base pressure of 5×10^{-2} mbar during the deposition. A high vacuum turbopump is used to achieve and maintain this low pressure. The separation between the target and substrate was 11cm. The post-annealing of undoped ZnO and AZO thin films is done in the oxygen environment for 1hr at 600^0C using a microprocessor-controlled furnace (GERO HRTH 40100/17, Nabertherm). This annealing is carried out to get thin films with good crystallinity and improved stoichiometry.

The crystallinity and structure of undoped ZnO and AZO thin films have been characterized at room temperature by using a glancing angle X-ray diffractometer (GAXRD), using Bruker D8 diffractometer with Cu-Ka X-ray (l- 1.54 Å) for 2θ range from 20^0 to 60^0 with a scan rate of 0.2/m. The structural studies were further done by the micro-Raman spectroscopy using a Renishaw In-Via Raman microscope. The 50mWArb ion laser in the 514.5 nm line is used to record the spectra. The microstructure and morphological investigations were done by a Scanning Electron Microscopy (SEM). Optical transmittance and absorbance spectra from 200 to 800 nm wavelength range were recorded using Hitachi UV 3300 double-beam spectrometer. The electrical transport

properties are studied by the two probe method. The FTIR spectroscopy is employed to characterise the functional groups, vibrational properties, defect and impurities of the synthesized materials. The FTIR setup from Bruker (VORTEX70) is used for the measurement in the range of 200-4000 cm^{-1}.

3. Results and discussions

3.1 Structural properties

In the present study, the thin films prepared by sputtering technique with different targets and are highly textured. The GAXRD patterns of the undoped, 1%AZO and 2%AZO thin film samples are represented in figure1. The X'pert high score software is used to appraise the recorded pattern. The peaks are indexed to the ZnO wurtzite structure (JCPDS card No. 36-1451). The pattern confirms the polycrystalline nature of the ZnO thin films with major diffraction from (002) peak with a c-axis orientation perpendicular to the substrate. The absence of the metallic peaks corresponding to the Zn or Al confirms the dopant is well substituted on the host site without causing much stress in the deposited thin films.

The preferred c-axis orientation of the thin film can be explained by the model "survival of the fastest" proposed by Drift (Van der Drift, 1967). The model explains that in the initial stage of deposition the nucleation of the various orientation is expected to be formed and every nucleus strives to grow but the nuclei with fastest growth rate can persist, i.e., c axis orientation is realized in ZnO. The pattern reveals the presence of weak (102) peak, which evolve in 2%AZO thin films as compared with undoped ZnO thin films. In 2%AZO thin film, sample have a mixed orientation with additional (100) and (101) peak of ZnO wurtzite structure.

Table 1: Full width at half maxima (FWHM), Crystallite Size (D), Dislocation density (δ), Strain (ε), Stress (σ) and Lattice parameter (c) for 1%AZO and 2%AZO thin film sample.

Sample	FWHM (002)	D(nm)	δ (10^{14} lines m^{-2})	Strain ε(10^{-4})	Stress σ(GPa)	Lattice parameters c(Å)
Undoped ZnO	0.336	24.7	16.3	58.8	-0.137	5.209
1% AZO	0.312	26.6	14.1	57.7	-0.135	5.209
2%AZO	0.336	24.7	16.3	-136.2	0.317	5.198

The (002) reflection peak position for the deposited thin films is close to the standard value (34.47^0) for ZnO powder. The effect of Al doping concentration can be seen with a

shift in the (002) peak position from 34.44^0 to 34.50^0 for the 1%AZO and 2%AZO thin films. Part et al.,(Kim et al., 1997) also witnessed the shift in (002) peak towards the higher value similar to our observations. This shift can be attributed to the difference in the ionic radii of the host Zn^{2+} (0.74Å) and dopant Al^{3+} (0.54Å), which causes the shortening of the c-axis. The value of the lattice parameter c has been calculated for undoped ZnO, 1%AZO and 2%AZO thin films and tabulated in Table1. The lattice parameter is calculated by using the following formula(Kaur et al., 2015)

$$c = \frac{\lambda}{sin\theta_{(002)}} \quad 1$$

These values are used for the clear estimation of the strain and stress in the thin film induced by the shortening of the c axis. The induced microstrain (ε) of the thin films have been calculated using the following formula(Yilmaz et al., 2016):

$$\varepsilon = \frac{\beta}{4tan\theta} \quad 2$$

Where β is FWHM and θ is Bragg's angle. For the AZO thin films the c-axis stress is calculated by employing the biaxial strain model(Jo et al., 2018):

$$\sigma = \frac{2c_{13}^2 - c_{33}(c_{11}-c_{12})}{2c_{13}} \times \varepsilon \quad 3$$

Where, $c_{11}, c_{12} c_{13}$ and c_{13} are the elastic constants of a single crystal having the values 208.8, 114.7, 104.2 and 213.8 respectively. Equation (3) can be simplified to

$$\sigma = -233 \times \varepsilon(GPa).$$

The micro-strain and stress value of the thin films are tabulated in Table1, the value first decreases for the 1%AZO sample and then increase for the 2%AZO sample. The positive sign of stress value refers to the tensile and negative sign for compressive stress(Jo et al., 2017). For undoped and 1%AZO thin films, compressive stress is observed on the other hand tensile stress is obtained in the case of 2%AZO thin film. The augmented stress values, increase the light scattering in the 2%AZO thin films and thus affecting the optical properties.

The FWHM of (002) peak, obtained from the XRD pattern are listed in Table2. The FWHM decrease for 1%AZO sample and then increases for 2%AZO thin films as compared with undoped ZnO thin films. This result show improvement in the crystallinity for the 1%AZO thin film. The average particle size D is calculated using Scherrer's formula(Srinatha et al., 2017) from the (002) peak.

Table 2: Optical bandgap value of pristine and implanted sample1%AZO and 2%AZO

Al Conc.	Undoped ZnO	1%AZO	2%AZO
Bandgap(eV)	3.28	3.27	3.30

$$D = \frac{K\lambda}{\beta cos\theta} \quad 4$$

Where, K=0.9 is Scherer's constant which depends on the shape of crystallite, λ=1.5418 Å, is X-ray wavelength for Cu Kα target, β is FWHM for (002) peak and θ is the Bragg's angle (half of the peak position angle). As the D value is calculated from the FWHM value it shows a similar trend with variation in Al dopant concentration. An increase in crystallite size for 1%AZO sample is a signature of reduction in ZnO stoichiometry by substitutional replacement of Zn with Al which is in harmony with the absence of any metallic phase. The variation in lattice parameter c with Al doping concentration from 1% to 2% alters the shape of the crystallite and can also be related to the variation in D value. This trend can be an outcome of the misfit stress that impose a negative effect on the structural factors of the thin films. The presence of the geometric mismatch between the deposited thin film and substrate is also responsible for these results.

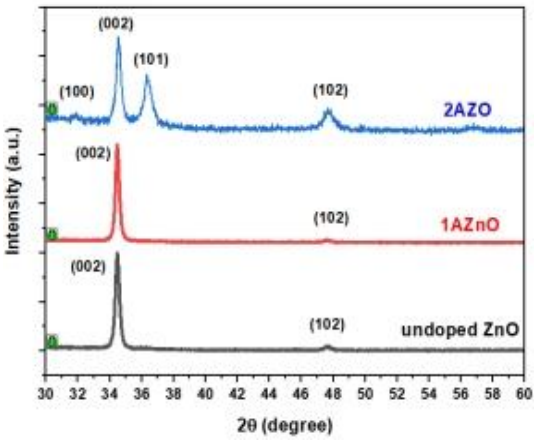

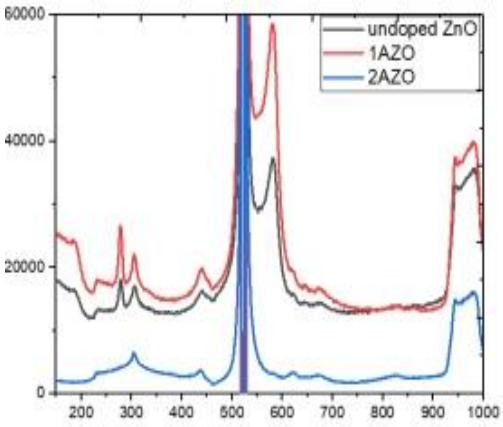

Figure 1: The XRD patterns of the undoped, 1%AZO and 2%AZO thin film samples
Figure2: Micro-Raman spectra of undoped ZnO and AZO thin films

The length of dislocation lines per unit volume known as the dislocation density gives the extent of the defects in the crystal. The dislocation density (δ)has been estimated by employing the following formula(Yilmaz et al., 2016)

$$\delta = \frac{1}{D^2} \qquad 5$$

The values, given in Table1, decrease slightly for the 1%AZO sample and then increases for 2%AZO thin films as compared with undoped ZnO thin films. The result indicates the increment of the defects in the crystal structure.

3.2 Raman Studies

Zinc oxide in wurtzite structure is in space group C_V^6. The irreducible representation for the optical phonons in the Brillouin zone is given by Damen et al., 1966(Damen et al., 1966)

$$\Gamma_{optical} = A_1 + 2E_2 + E_1 \qquad 6$$

where, E_1 and A_1 both are polar modes that split into longitudinal optical and transverse optical (TO), in the presence of macroscopic electric field related to (LO) phonons. The

micro-Raman spectra of undoped ZnO and AZO thin films are shown in Figure2. The spectra consist of peaks at 440 and 580 cm^{-1}, which are assigned to vibrational mode E_2 (high) and E_1 (LO) mode. The peak present at 306 and 522 cm^{-1} are due to Si substrate and emerged by two phonon modes and second-order processes. The presence of this signal is due to lower film thickness than the penetration depth (512 nm) of the laser. These peaks are attributed to the combined (TO and TA) phonon modes 9 of Si. All the observed peaks of Raman spectra are within the error limit.

It is noteworthy that the profile and position of the Raman peak influenced by the presence of residual stress, crystallization, crystal defects and structural disorder in the thin film. The oxygen sublattice and wurtzite structure of ZnO is confirmed by E_2 (high) mode(Gautam et al., 2014). The peak assigned for E_2 (high) mode persists in all the samples indicating the stable polycrystalline nature. The intensity is suppressed for a 2%AZO sample showing the gradual increase of defect density (oxygen vacancies) with increasing Al concentration in ZnO thin films. The minute red shift in the frequency with a suppressed intensity of E2 mode can be correlated to the induced stress in the host lattice calculated by XRD results. The Raman peak emerging at 580 cm^{-1} is designated for E_1(LO) mode in undoped ZnO and 1%AZO thin films attributed to intrinsic defects (V_O and Zn_i) present in host ZnO. This E_1(LO) mode is absent in 2%AZO thin film. The spectra indicate the presence of anomalous vibrational mode at 277 cm-1 undoped ZnO and 1%AZO sample whereas absent in 2%AZO sample. This mode is present in nitrogen-doped ZnO. By theoretical calculation, Wang et al(Wang et al., 2006), suggest that this mode is due to vibrations of Zn adjacent to the O atoms that are replaced by the dopant N atom. However, the exact verification for the origin of this mode in our system still needs to be investigated.

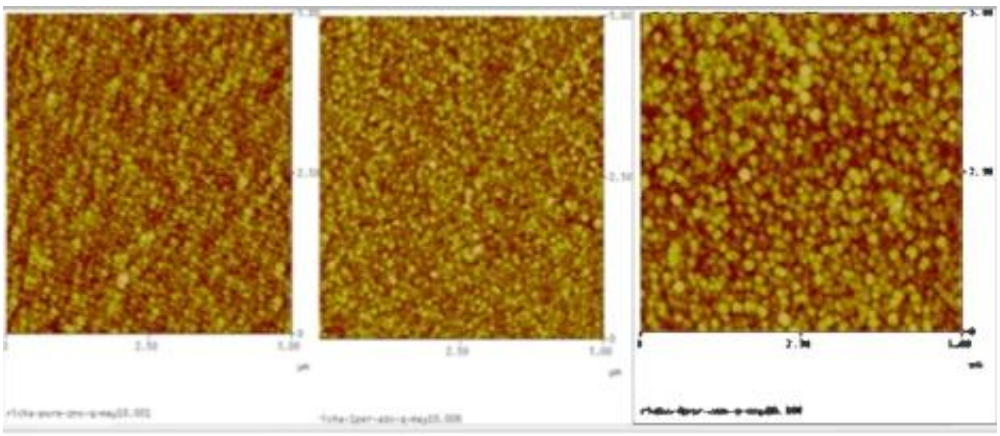

Figure 3: 2D AFM micrograph of (a) Undoped (b) 1%AZO and (c) 2%AZO thin film

Morphological Studies

Atomic force microscopy is used to study the microstructure and morphology of the surface of the deposited thin films. The tapping mode AFM micrographs gives a comparison of undoped ZnO and AZO thin films are shown in Figure3.The dense grainy morphology with increased grain size for 2%AZO thin films. The topography of the undoped ZnO thin film is a relatively smooth and of good quality in contrast with the other thin films with increasing Al (1 and 2 wt%) amount. The surface roughness value shows a significant increase for 1%AZO thin film (8.811 nm) and an increase in the case of 2%AZO (7.404 nm) thin film in comparison to undoped ZnO (6.158 nm) thin films. The spherical shape grains in Undoped ZnO thin films get distorted which is attributed to increasing Al (1 and 2 wt %) amount for 1%AZO and 2%AZO thin films. These results are also consistent with the XRD results. The surface morphologies show a clear and noticeable change with Al doping. Figure3 shows that the undoped ZnO thin film entails consistent and symmetrical spherical crystallites of uniform size in contrast to distorted spheres in the case of AZO thin films.

This change in the crystallite shape may be attributed to the transition of compressive stress to tensile stress in the case of undoped ZnO and 2%AZO thin films respectively. With an upsurge in Al concentration from 1wt% to 2wt%, the grains grow into more of a random shape. The films become more densely packed without any cracks on the surface. Larger grains are observed for 2%AZO thin film. The particle size has been calculated from FE-SEM micrographs (Figure 4). The average particle size is about 46, 67 and 83nm for undoped, 1%AZO and 2%AZO thin films respectively. The trend of increase in particle size is in harmony with the XRD results but as expected XRD analysis underestimated the crystallite size. Thus we can say that the concentration of dopant affects the morphology of the thin films.

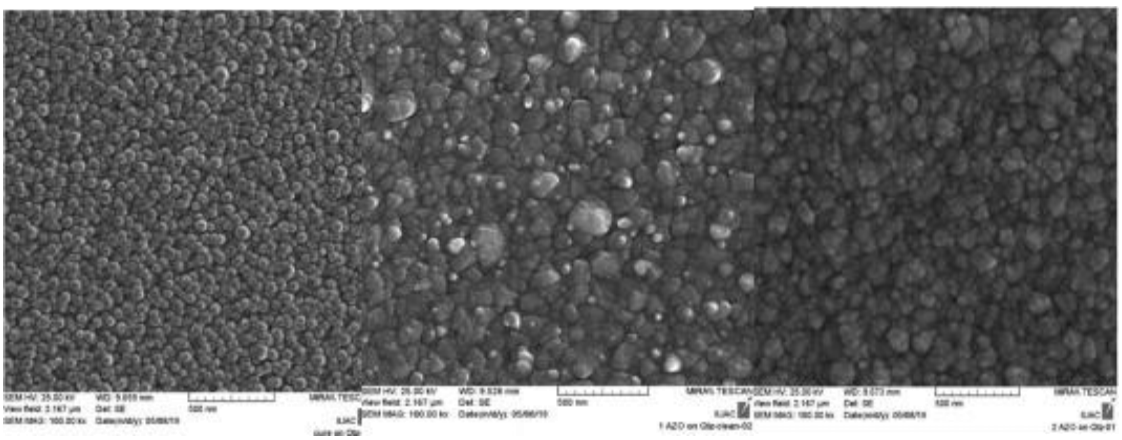

Figure4: FE- SEM micrograph of (a) Undoped (b) 1%AZO and (c) 2%AZO thin film

Optical Studies

In order to study the effects of Al dopant concentration on the optical properties of the AZO thin films, the UV-Vis spectrophotometer is employed to record the optical transmittance and absorbance spectra. The Transmittance spectra are depicted in Figure 5. Particularly all the deposited thin films are transparent in the visible region with average transmittance lies between 80-90%. The transmittance pattern shows an interference pattern originating due to the interference of light at the boundary of the substrate and deposited films which verifies the smoothness of the deposited thin films. The transmittance of the 1%AZO sample decrease significantly which further increase for 2%AZO thin films. This change in the transmittance can be attributed to the variation in Al dopant concentration and particle size, witnessed by the other characterization method.

In semiconductors the optical transitions information (optical band gap) can be extracted from the basic absorbance spectra by the optical method and illustrated in figure6. The optical bandgap is calculated using Tauc's equation(Tauc et al., 1966)

$$\alpha h\nu \approx C(h\nu - E_g)^{1/2} \qquad 7$$

where C is a constant, α is the absorption coefficient, ν is the photon energy and 1/2 is for the direct transitions. The values are tabulated in Table 2. With reference to deposited undoped ZnO thin films the bandgap of 1%AZO thin-film decrease slightly and increase with increased Al concentration for 2%AZO thin film. The obtained values of optical bandgap are in harmony with the values in the literature despite the various thin film deposition method. The increase in the bandgap value with increased Al concentration can be understood by increased carrier concentration. In the substitution of host Zn^{2+} ions by Al^{3+} dopant ion, an extra free electron is available which occupy the energy levels that lies below the conduction band. It is a well-known fact that an augmentation in the optical band gap of the metal oxide semiconductor is observed with increasing carrier concentration and is well explained by the BM effect.

In contrast, there are some other factors such as the crystallite size, phase purity internal stress etc. which influence the optical band gap and may responsible for the observed decrement in the case of 1%AZO thin film(Zhu et al., 2011). It can be concluded by the observed results that the bandgap can be controlled by altering the Al concentration.

Electrical Transport Studies

In semiconductors, mobility is an imperative factor as it explains the movement of the particle in the electric field. The n-types conductivity, in ZnO, arises due to the oxygen vacancies and Zinc interstitials. The Undoped ZnO thin films prepared by RF sputtering method are highly resistive and does not show ohmic behaviour in the I-V curve.

On the other hand, the AZO(1% and 2%) thin films are n-type conductive with ohmic nature measured by using Keithley two

probe set up and are shown in Figure7. The mean resistivity value of 1%AZO and 2%AZO thin-film is1.48×10^{8} ohm and 2.58×10^{9} ohm respectively. The effective substitution of Al dopant ion reduces the strained bonds and dangling between the Zinc ion and oxygen vacancies, which in turns reduce the resistivity value of 1%AZO thin film as compared to undoped ZnO. This substitution also increases the carrier concentration in the thin films resulting in an improvement in the conductivity.

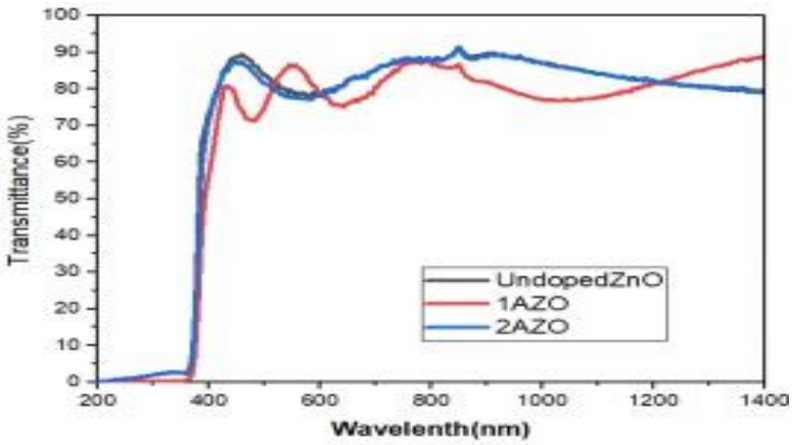

Figure 5: Transmission curve of undoped and AZO thin films

The Al dopant (donor Al^{3+} cation) shifts the Fermi level of AZO thin films to the higher position into the conduction band due to which completely degenerate films are obtained. The preferred c-axis (002) orientation as observed by the XRD pattern of the thin films also collaborates with the resistivity values. The 1%AZO thin films have lower resistivity value owning to the crystalline nature and more preferable c- axis (002) orientation as compared to the 2%AZO thin films. These results are well reported in literature(Srinatha et al., 2017). The lower resistivity value for 1%AZO thin films can be understood by reduced lattice defect that is also confirmed by XRD results and increased scattering of carrier electron from the grain boundaries. The free charge electrons can be trapped by the grain boundaries and a potential barrier is formed, which scatters the conduction electrons. This scattering results in the accumulation of negative charge which increases the resistivity value in 2%AZO thin films. Apart from the crystal orientation the crystallite size also affects the resistivity of the thin film. This trend shown by the resistivity values can easily be correlated with the crystallite size calculated by XRD data. As the crystallite size increases it reduces the grain boundaries causing the decrement in the resistivity. The change in grain size can also be observed from the SEM images and shows the same trend.

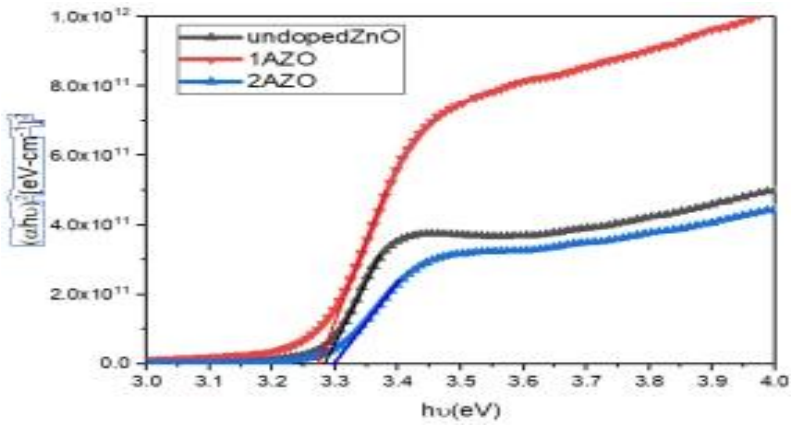

Figure 6: Tauc plot of undoped and AZO thin film

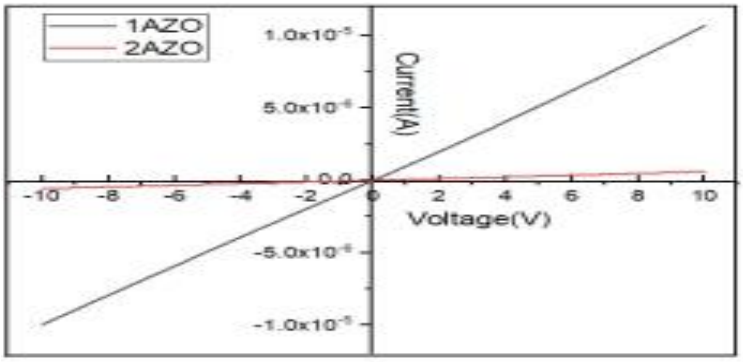

Figure 7: I-V plot of 1%AZO and 2%AZO thin film sample

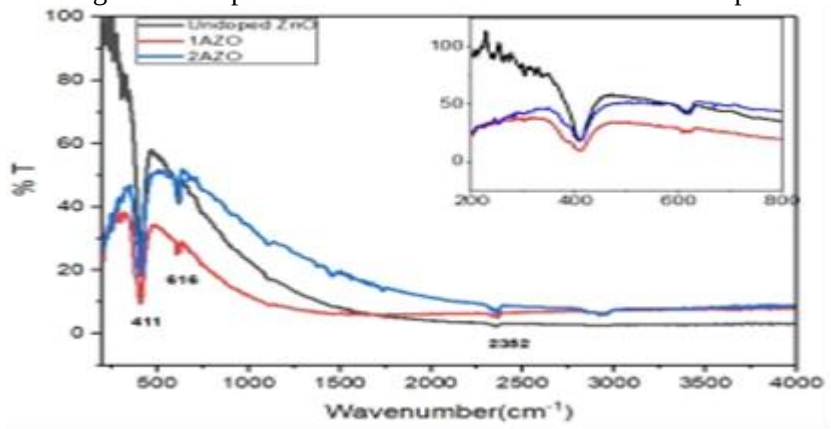

Figure 8: FTIR spectrum of Undoped ZnO, 1%AZO and 2%AZO thin films

FTIR Studies

Fourier-transform infrared spectroscopy (FTIR) is a useful technique to characterise the functional groups, vibrational properties, defect and impurities of the synthesized materials. The structure, morphology and chemical composition of the thin films decides the position of the absorption peak and band position. Figure8 shows the FTIR spectrum of Undoped ZnO, 1%AZO and 2%AZO thin films recorded in the range. In the IR spectrum, a signature peak is observed at 411

cm^{-1} for the undoped ZnO and AZO thin films and corresponds to the ZnO bond stretching in tetrahedral coordination.

Broadening in the peak is observed due to the doping effect which may be attributed to the stress caused by the Al ion. The stretching vibrations of Zn-O bonds present in octahedral coordination originate the peaks around $617cm^{-1}$. Although these peaks are present in the spectrum but are not as prominent as peaks originated by the tetrahedral coordination of ZnO which further confirms the wurtzite structure of the deposited thin film sample. This FTIR observation is in harmony with the XRD analysis of the samples. The position and broadness of the signal at $617cm^{-1}$ is not much affected by the doping concentration, therefore it confirms that the substitution of Zn ion by the Al ions in the tetrahedral arrangement. A weak peak at $1102cm^{-1}$ is due to the substrate Si-O-Si bonds. In a 2%AZO thin film sample, a weak peak is observed at 1458 cm^{-1} assigned to the symmetrical C=O stretching of zinc carboxylate due to Lewis acidity(Sharma and Jha, 2017). The atmospheric CO_2 absorption gives rise to the peak at $2373cm^{-1}$. A broadband at 2922 cm^{-1} can be observed in 2%AZO thin-film originating due to the presence of CH. The presence of these band can be related to the absorbed group on the thin film surface and does not reflect the contaminations.

Conclusion

The undoped ZnO, 1%AZO and 2%AZO thin films are deposited on quartz substrate by using RF magnetron sputtering. XRD results confirm the presence of highly textured and polycrystalline ZnO thin films with preferential c-axis orientation. The result indicates that as we increase Al concentration in ZnO the nature of stress is changed, which in turn affect the optical properties. The crystallinity of the thin film is enhanced but at the same time, the number of defects is also increased in the thin film. Raman study indicates that the profile and position of the Raman peak are influenced by the alteration in residual stress, crystallization, crystal defects and structural disorder that is present in the thin film. The percentage of Al content clearly affects the surface roughness that is depicted in AFM analysis. The increase in particle size calculated from FE-SEM is consistent with the crystallite value calculated in XRD analysis. The average transmittance of all the thin films is 80-90% in the visible region. The increase in optical bandgap under different doping percentage is explained by the BM effect. The ohmic behaviour of doped thin film is observed by two probe setup. The resistivity value is altered with Al doping. The presence of different functional groups, defects and impurities is confirmed by FTIR. The results clearly show that the introduction of Al dopant alters the various ZnO material properties.

Acknowledgements

The authors are grateful to the Director, Inter University Accelerator Centre, New Delhi for providing support throughout the experimental work. The authors are also thankful to Dr

Pawan Kularia, Dr S.A. Khan and Dr Indira Sulani for experimental support. One of the authors (RS) is also thankful to UGC for providing the financial support under the scheme of PhD student fellowship.

References

Damen, T.C., Porto, S.P.S., Tell, B., 1966. Raman effect in zinc oxide. Phys. Rev. 142, 570.

Gautam, S.K., Singh, F., Sulania, I., Singh, R.G., Kulriya, P.K., Pippel, E., 2014. Micro-Raman study on the softening and stiffening of phonons in rutile titanium dioxide film: Competing effects of structural defects, crystallite size, and lattice strain. J. Appl. Phys. 115, 143504.

Granqvist, C.G., 2000. Electrochromic tungsten oxide films: review of progress 1993–1998. Sol. Energy Mater. Sol. Cells 60, 201–262.

Jo, G.H., Kim, S., Koh, J., 2017. Enhanced electrical and optical properties based on stress reduced graded structure of Al-doped ZnO thin fi lms Al doping d co tion (mol %. Ceram. Int. 0–1. https://doi.org/10.1016/j.ceramint.2017.09.240

Jo, G.H., Kim, S.H., Koh, J.H., 2018. Enhanced electrical and optical properties based on stress reduced graded structure of Al-doped ZnO thin films. Ceram. Int. 44, 735–741. https://doi.org/10.1016/j.ceramint.2017.09.240

Kaur, G., Mitra, A., Yadav, K.L., 2015. Influence of Beam Energy on the Properties of Pulsed Laser Deposited Al-Doped ZnO Thin Films. IEEE Trans. Nanotechnol. 14, 922–930. https://doi.org/10.1109/TNANO.2015.2463085

Kim, K.H., Park, K.C., Ma, D.Y., 1997. Structural, electrical and optical properties of aluminum doped zinc oxide films prepared by radio frequency magnetron sputtering. J. Appl. Phys. 81, 7764–7772. https://doi.org/10.1063/1.365556

Lee, J.H., Park, B.O., 2004. Characteristics of Al-doped ZnO thin films obtained by ultrasonic spray pyrolysis: Effects of Al doping and an annealing treatment. Mater. Sci. Eng. B Solid-State Mater. Adv. Technol. 106, 242–245. https://doi.org/10.1016/j.mseb.2003.09.040

Malek, M.F., Mamat, M.H., Sahdan, M.Z., Zahidi, M.M., Khusaimi, Z., Mahmood, M.R., 2013. Influence of various sol concentrations on stress/strain and properties of ZnO thin films synthesised by sol–gel technique. Thin Solid Films 527, 102–109.

Peiró, A.M., Ravirajan, P., Govender, K., Boyle, D.S., O'Brien, P., Bradley, D.D.C., Nelson, J., Durrant, J.R., 2006. Hybrid polymer/metal oxide solar cells based on ZnO columnar structures. J. Mater. Chem. 16, 2088–2096.

Sharma, D., Jha, R., 2017. Analysis of

structural, optical and magnetic properties of Fe/Co co-doped ZnO nanocrystals. Ceram. Int. 43, 8488–8496. https://doi.org/10.1016/j.ceramint.2017.03.201

Srinatha, N., Raghu, P., Mahesh, H.M., Angadi, B., 2017. Spin-coated Al-doped ZnO thin films for optical applications: Structural, micro-structural, optical and luminescence studies. J. Alloys Compd. 722, 888–895. https://doi.org/10.1016/j.jallcom.2017.06.182

Tauc, J., Grigorovici, R., Vancu, A., 1966. Optical properties and electronic structure of amorphous germanium. Phys. status solidi 15, 627–637.

Van der Drift, A., 1967. Evolutionary selection, a principle governing growth orientation in vapour- deposited layers. Philips Res. Rep 22, 267.

Wang, J.B., Zhong, H.M., Li, Z.F., Lu, W., 2006. Raman study of N+-implanted ZnO. Appl. Phys. Lett. 88, 101913.

Yilmaz, M., Tatar, D., Sonmez, E., Cirak, C., Aydogan, S., Gunturkun, R., 2016. Investigation of Structural, Morphological, Optical, and Electrical Properties of Al Doped ZnO Thin Films Via Spin Coating Technique. Synth. React. Inorganic, Met. Nano-Metal Chem. 46, 489–494. https://doi.org/10.1080/15533174.2014.988795

Zhu, B.L., Wang, J., Zhu, S.J., Wu, J., Wu, R., Zeng, D.W., Xie, C.S., 2011. Influence of hydrogen introduction on structure and properties of ZnO thin films during sputtering and post- annealing. Thin Solid Films 519, 3809–3815.